Persistent α1-adrenergic receptor function in the nucleus locus coeruleus causes hyperexcitability in AD/HD model rats

Sachiyo Igata[1,3], Tokumasa Hayashi[2], Masayuki Itoh[1], Takashi Akasu[4], Makoto Takano[1], and Masaru Ishimatsu[1]

[1]Department of Physiology, Kurume University School of Medicine and [2]Department of Urology, 67 Asahi-machi, Kurume 830-0011, Japan

[3]Department of Health Sciences, Faculty of Medical Sciences, Kyushu University, 3-1-1 Maidashi, Higashi-ku, Fukuoka 812-8582, Japan

[4]Institute of Cognitive Brain Diseases, Shinwakai Kyoritsu Hospital, 3-42 Nakagawara-machi, Nobeoka 882-0031, Japan

Running Head: Functional α1-AR in nucleus locus coeruleus in SHR

Corresponding author: Masaru Ishimatsu

Department of Physiology, Kurume University School of Medicine, 67 Asahi-machi, Kurume 830-0011, Japan

Tel: +81 942-31-7543; Fax: +81 942-31-7728; Email: masaruster@gmail.com

Abstract

Spontaneous hypertensive rats (SHR) are widely used as a model of attention deficit hyperactivity disorder (ADHD) as their ADHD-like behaviors are restored by methylphenidate (MPH). However, a postnatal neural development in SHR is unknown. We performed whole cell patch clamp recordings from locus coeruleus (LC) neurons in neonatal (P 3–5), juvenile (P 21–28) and adult (P 49–56) SHR and age-matched Wistar rats to evaluate α1- and α2-adrenergic receptor (ARs) activities at each developmental period. LC neurons in neonatal Wistar rats and SHR showed no difference in resting membrane potential (RMP) and spontaneous firing rate (SFR), while juvenile and adult SHR LC neurons showed depolarized RMP and faster SFR than in Wistar rats. Blockade of α1-AR activity by prazosin hyperpolarized the membrane and abolished spontaneous firings in all developmental periods in SHR LC neurons, but not in juvenile and adult Wistar rats. α1-AR stimulation by phenylephrine (PE) evoked an inward current in juvenile LC neurons in SHR, but not in juvenile Wistar rats. This PE-induced inward current was abolished by non-selective cation channel blockers. By contrast, α2-AR stimulation-induced outward currents in the presence of an α1-AR antagonist were equivalent in SHR and Wistar LC neurons. These data suggest that Wistar LC neurons lose α1-AR function during development, whereas α1-ARs remain functional in SHR LC neurons. Thus, persistent intrinsic activity of α1-ARs may be a neural mechanism contributing to developmental disorders in juvenile SHRs.

Keywords: locus coeruleus, adrenergic receptor, spontaneously hypertensive rat, ADHD, noradrenaline

Introduction

The functional role of α1- and α2-adrenergic receptors (ARs) is a focus of cognitive and sustained attention in attention deficit hyperactivity disorder (ADHD). The α1- and α2-ARs have opposing effects on cognitive function in prefrontal cortex neurons in Sprague-Dawley (SD) rats. Activation of α2-ARs improves working memory performance in rats, whereas high levels of noradrenalin release impair cognitive function through actions at α1-ARs (Arnsten et al. 2007; Birnbaum et al. 1999). This α1-AR activation is considered necessary for methylphenidate (MPH)-induced improvement in sustained attention in SD rats (Berridge et al. 2012; Osborne et al. 2002).

The nucleus locus coeruleus (LC) is the major noradrenergic nucleus of the brain, and provides the noradrenergic projections to multiple brain areas including the prefrontal cortex (Aston-Jones et al. 1991; Foote et al. 1980). Resting membrane potential and a pattern of spontaneous firing in LC neurons are associated with arousal and vigilance, and are potentially affected by α1- and α2-AR activation (Aston-Jones and Bloom 1981a, 1981b; Aston-Jones and Cohen 2005; Foote et al. 1980; Howells et al. 2012). Application of clonidine to rat LC neurons activates a class of G-protein coupled inwardly rectifying potassium (GIRK) channels via the α2-AR, resulting in membrane hyperpolarization and inhibition of the spontaneous firing of the action potentials (APs) (Aghajanian and VanderMaelen 1982; Arima et al. 1998; Williams et al. 1985, 1988). By contrast, Williams and Marshall (1987) reported that α1-AR agonists such as phenylephrine (PE) induced membrane depolarization and accelerated spontaneous firing rates by activating unknown cation channels in neonatal rat LC

neurons. While α1-ARs are known to couple with a Gq protein, it remains unclear what cationic channel is involved in the PE-induced membrane depolarization. Moreover, they reported that the effects of α1-AR on membrane potential were only detected in LC neurons from neonatal rats, but not from older rats (> P21). These studies suggest that the activities of LC neurons under control of both α1- and α2-ARs could be altered during postnatal developmental periods (neonatal, juvenile and adult).

The spontaneously hypertensive rat (SHR) is the most widely used animal model of ADHD (Adriani et al. 2003; Russell 2007; Sagvolden 2000; Sagvolden et al. 1993). A juvenile SHR (P21–28) starts to display behaviors characteristic of ADHD with no hypertension, which can be restored by intra-abdominal injection of therapeutic agents such as MPH (Adriani et al. 2003). Although there are several behavioral studies using SHR, electrophysiological studies using brain slice preparations are limited. In particular, SHR LC activities in the different developmental periods are critical to understanding local neural communication in developmental disorders. In the present study, we evaluated the α1- and α2-AR contribution to the membrane properties of LC neurons using neonatal, juvenile, and adult SHR and compared them with age-matched Wistar rats. We also explored the unknown cationic channel activated by α1-AR stimulation.

Methods

Slice Preparation

All experimental procedures were approved by the Institutional Animal Use and Care Committee of Kurume University School of Medicine and were performed in accordance with the guiding principles of the Physiological Society of Japan. All animals were housed in a controlled environment room under a 12:12 h light-dark cycle with free access to food and water. Male Wistar rats and SHRs during postnatal day 3–5 (P3–5), postnatal day 21–28 (P21–28) and postnatal day 49–56 (P49–56) were decapitated under pentobarbital sodium anesthesia (50 mg/kg, i.p.). The brains were quickly removed and immersed for 8–10 s in a cooled sucrose artificial cerebrospinal fluid (ACSF, 4–6 °C) that was prebubbled with 95% O_2-5% CO_2. Horizontal brain slices (240 μm thick) were cut with a vibrating microtome (VT1000s; Leica, Wetzlar, Germany) in cooled sucrose ACSF. The sucrose ACSF was composed of 199 mM sucrose, 2.5 mM KCl, 2.4 mM $MgCl_2$, 23.8 mM $NaHCO_3$, 12.5 mM $NaHPO_4$ and 10 mM D-glucose. Brain slices were left to recover for 1 h in oxygenated normal ACSF at 32 °C. A hemisected slice was then transferred to a recording chamber and submerged in the normal ACSF at 32–34 °C with a perfusion rate of 2.5 ml/min. The composition of the normal ACSF was 126 mM NaCl, 2.5 mM KCl, 2.4 mM $CaCl_2$, 1.2 mM $MgCl_2$, 21 mM $NaHCO_3$, 1.2 mM $NaHPO_4$ and 11 mM D-glucose (pH 7.4, 279–288 mOsm).

Electrophysiological Recordings

Whole cell recordings were made from LC neurons using the slice patch technique. Patch pipettes were prepared from borosilicate glass capillaries with a micropipette puller (PP83; Narishige, Tokyo, Japan). Patch pipettes were filled with an internal solution of 140 mM K-gluconate, 10 mM NaCl, 0.3 mM $CaCl_2$, 1 mM $MgCl_2$, 1 mM

EGTA, 0.25 mM GTP and 10 mM HEPES (pH 7.3 adjusted by KOH, 280–285 mOsm). The tip resistance of the whole cell patch pipette was 3–5 MΩ. The liquid junction potential of −10.8 mV for K-gluconate was corrected. Whole cell recordings were sampled at 10 kHz using an Axopatch 200B amplifier (Axon Instruments, Sunnyvale, CA, USA). Spontaneous APs and resting membrane potential (RMP) were recorded from LC neurons using the whole cell current-clamp mode. Voltage clamp was analyzed at a holding potential (Vh) of -60 mV. Membrane potential and current were filtered at 1 kHz for analysis with pClamp software (Axon Instruments). The drugs used in the present study were guanosine 5'- triphosphate sodium salt hydrate (GTP), ethylene glycol-bis (2-aminoethylether)-N,N,N',N'-tetraacetic acid (EGTA), epinephrine (noradrenaline; NA), yohimbine, prazosin, phenylephrine (PE), 2-aminoethyl diphenylborinate (2-APB), flufenamic acid (FFA), methylphenidate (MPH) (Sigma, St. Louis, MO, USA), $BaCl_2$ (Wako, Tokyo, Japan) and tetrodotoxin (TTX) (Nacalai Tesque, Kyoto, Japan). Yohimbine, prazosin, 2-APB and FFA were dissolved in dimethyl sulfoxide (DMSO), with a final concentration of 0.02% DMSO.

Immunohistochemistry in LC

Six rats were anesthetized and transcardially perfused with heparinized saline followed by 300 ml of 4% paraformaldehyde (PFA) in 0.1 M phosphate buffer (PB, pH 7.4). Each brain was removed and a section containing the LC was cut and post fixed in 4% PFA at 4 °C for 18 h. The section was cryoprotected in 0.1 M PB containing 30% (w/v) sucrose for 18 h. The horizontal section was further cut into 70-μm-thick slices on a freezing microtome. The slices were incubated in 5% normal donkey serum for 1 h at room temperature (RT). Free-floating slices were incubated with a polyclonal rabbit anti-α1A-adrenoceptor antibody (1:200; Alomone, Jerusalem, Israel), a polyclonal

rabbit anti-α2B-adrenoceptor antibody (1:200; Alomone) or a monoclonal anti-tyrosine-hydroxylase antibody (1:2000; Sigma) for 24 h at 4 °C in phosphate-buffered saline (PBS) containing 0.5% (v/v) triton (TM) X-100, 1% (w/v) bovine serum albumin and 0.1% (w/v) NaN_3. After several rinses in PBS, the slices were incubated in Alexa Fluor® 488 Goat Anti-Rabbit IgG (1:1000; Invitrogen, Carlsbad, CA, USA) and Alexa Fluor® 568 Goat Anti-Mouse IgG (1:500; Invitrogen) for 4 h at RT. Nuclei were stained using DAPI reagent for 1 h at RT. After washing, the specimens were mounted using PermaFluor aqueous mounting medium (Thermo, Fremont, CA, USA). The preparations were examined on a FluoView 1000 laser scanning confocal microscope system (Olympus, Tokyo, Japan). The controls included omission of the primary antibody.

Statistical Analyses

Each experimental value was presented as the mean±SE, and data were analyzed by unpaired Student's *t*-test. All statistical comparisons were made using Prism version 4 software (GraphPad, San Diego, CA, USA). *P* values <0.05 were considered statistically significant.

Results

To examine LC neuron membrane properties during postnatal development, we compared the RMP and spontaneous firing rate (SFR) at three developmental time points, P 3–5 (neonatal), P 21–28 (juvenile) and P 49–56 (adult), using a whole cell patch clamp technique (Fig. 1). Neonatal RMP was −54.8±0.8 mV and −53.5±1.0 mV in Wistar rats (*n*=10) and SHR (*n*=8), respectively. The SFR was 0.95±0.23 Hz and 1.05±0.56 Hz in Wistar rats (*n*=10) and SHR (*n*=8), respectively (Fig. 1*A*). In juvenile animals, RMP was −57.4±0.7 mV (*n*=18) in Wistar rats and −53.1±1.2 mV (*n*=19) in SHR, and SFR was 0.57±0.06 Hz (*n*=18) in Wistar rats and 1.23±0.17 Hz (*n*=19) in SHR (Fig. 1*B*). In adult animals, RMP was -57.2±0.6 mV (*n*=12) in Wistar rats and -54.3±0.9 mV (*n*=12) in SHR, and SFR was 0.65±0.16 Hz (*n*=12) in Wistar rats and 1.7±0.13 Hz (*n*=12) in SHR (Fig. 1*C*). In the neonate, RMP and SFR were not statistically different between SHR and Wistar rat LC neurons, while RMP was significantly depolarized ($P<0.01$) and SFR was significantly faster ($P<0.01$) in SHR LC neurons in the juvenile and adult periods when compared with age-matched Wistar rat. Both α1- and α2-ARs are known to be involved with RMP of LC neurons via a cation channel and an inwardly rectifying potassium channel, respectively. Williams and Marshall (1987) reported that an inward current coupled with α1-ARs is a characteristic membrane property in neonatal LC neurons.

Next, we examined a possible involvement of α1-ARs in the membrane potential in juvenile and adult rat LC neurons. First, we tested the effect of prazosin on RMP and spontaneous firing. Prazosin (500 nM) induced membrane hyperpolarization and inhibition of spontaneous firing in neonatal rat LC neurons (Wistar: 5.5±0.7 mV, *n*=8; SHR: 5.9 ± 0.6 mV, *n*=8; *P*=0.58, Fig. 2*A*). Juvenile SHR LC neurons also exhibited

membrane hyperpolarization (6.9±0.7 mV, *n*=7), which was not observed in age-matched Wistar rats (*n*=6) (Fig. 2*B*). We also confirmed that LC neurons obtained from adult SHRs showed hyperpolarization by prazosin (6.3±0.8 mV, *n*=5), which was not observed in adult Wistar rats (*n*=7) (Fig. 2*C*). These results show that the membrane properties of juvenile and adult SHR are qualitatively equivalent. It was previously reported that SHR (> P35) become hypertension, which could alter a central and/or a peripheral catecholaminergic system. We performed the following experiments using neonatal and juvenile SHR. In neonatal rats, prazosin (500 nM) in the presence of TTX (1 μM) and yohimbine (1 μM) induced outward currents in LC neurons (Wistar: 13.8±1.3 pA, *n*=7; SHR: 17.2±2.1 pA, *n*=7; *P*=0.44, Fig. 3*A*). In juvenile rats, while prazosin also evoked an outward current (18.7±1.6 pA, *n*=7) in SHR LC neurons, Wistar LC neurons were not affected by prazosin (*n*=8) (Fig. 3*B*). Next, we tested the effect of PE, an α1-AR agonist. Bath application of PE (30 μM) in the presence of yohimbine (1 μM), an α2-AR antagonist, caused inward currents accompanied by an increase in the conductance in LC neurons in neonatal rats (Wistar: –20.2±0.5 pA, *n*=10; SHR: –22.9±1.4 pA, *n*=16; *P*=0.117, Fig. 4*A*) and in juvenile SHR (−17.9±1.4 pA, *n*=21). However, no juvenile Wistar LC neurons (*n*=15) showed an inward current by PE (Fig. 4*B*). A steady inward current with no obvious desensitization was observed by continuous application of PE (30 μM) up to 15 min in juvenile SHR LC neurons (data not shown). This PE-induced inward current was blocked by the α1-antagonist, prazosin (500 nM) (Fig. 5*A*).

An α1-AR is known to couple with Gq protein (Gq), which was reported to activate non-selective cation channels (NSCC) (Clapham 2003; Montell 2005). Thus, we examined whether the NSCC blockers 2-APB and FFA could abolish the

PE-induced inward current. When the PE-induced inward currents reached the maximum amplitude, addition of prazosin, 2-APB, or FFA to the superfusate solution successfully blocked the inward current in juvenile SHR LC neurons (Prazosin: 2.42±3.3 pA, *n*=8; 2-APB: 12.4±1.9 pA, *n*=9; FFA: 9.1±3.3 pA, *n*=8; Fig. 5*A* and *B*). These results suggest an involvement of NSCC via α1-AR activation on RMP in LC neurons in neonatal Wistar and SHR rats, and in juvenile SHR rats, but not in juvenile Wistar rats.

An inwardly rectifying potassium channel (GIRK) coupled to α2-ARs is known to contribute to RMP in rat LC neurons. To evaluate the amount of outward current via α2-AR under physiological conditions, we examined the role of α2-ARs on the membrane current of LC neurons from juvenile SHR and Wister rats. High-dose NA (>10 μM) induced a smaller outward current in juvenile SHR LC neurons compared with Wistar rats (Fig. 6*C*). Low-dose NA (3 μM) induced an inward current in juvenile SHR LC neurons only (−20.2±2.2 pA, *n*=6), but not in Wistar rats (*n*=10) (Fig. 6*A* and *B*). Dose-dependent effects of NA are illustrated in Figure 6*C*. NA (3 μM) evoked an inward current, while the NA (>3 μM) evoked an outward current in juvenile SHR LC neurons. By contrast, all juvenile Wistar neurons showed an outward current by NA (3–300 μM).

Surprisingly, NA (3–100 μM)-induced outward currents obtained in the presence of prazosin (500 nM), an α1-antagonist, were virtually equivalent between juvenile SHR and Wistar LC neurons (Fig. 6*D*). A larger outward current was obtained by NA (≥10 μM) in the presence of prazosin from juvenile SHR LC neurons. Additionally, the Ba^{2+}, GIRK inhibitor, sensitive NA current was identical in both SHR and Wistar juvenile LC neurons (data not shown). We also examined the effect of MPH (30 μM) on

the membrane current in LC neurons using whole cell voltage clamp recording at a Vh of −60 mV. All LC neurons from juvenile Wistar rats showed outward currents (36±5.01 pA, *n*=15). By contrast, bath application of MPH to juvenile SHR caused varied currents depending on the cells (-35 to +30 pA; mean±SE = -2.0±5.0 pA; *n*=15 from six rats); inward current in five cells, outward current in five cells, and no effect in five cells. Lower concentrations of MPH (1 μM) induced no obvious current in both Wistar and SHR (Fig. 6*E*).

Finally, we tested the possibility that α1-ARs of LC neurons were absent in juvenile Wistar rats using immunohistochemistry for α1A- or α2B-AR (green), tyrosine-hydroxylase (TH: red) and cell nuclei (blue). TH immunoreactivity in the region of the LC neurons is shown in Figure 7*a* and *d*. Two distinct α1A- and α2B-ARs were located within a field of dense TH positive neurons in both SHR and Wistar rats (Fig. 7*c* and *f*).

Discussion

In the present study we examined the membrane properties of LC neurons in SHR and Wistar rats at different postnatal developmental stages. SHR are widely used as an ADHD model animal as they display ADHD-like characteristic behaviors such as hyperactivity and impulsivity (Adriani et al. 2003; Russell 2007; Sagvolden 2000; Sagvolden et al. 1993) in the juvenile period (P21–28) before development of hypertension (> P35). In previous reports, the Wistar Kyoto rat (WKR) strain was used as a normotensive control strain for the SHR. However, the WKR was recently reported to represent a type of depression animal model (Andrus et al. 2012; Hurley et al. 2013; Yamada et al. 2013). Therefore, we used Wistar rats as control animals in the present study.

We explored the local neural mechanisms in LC underlying the developmental disorder in SHR. It was reported that the firing patterns of LC neurons are critical for attention and vigilance. Two firing patterns of LC neurons have been reported: phasic and tonic. Animals showed good performance in selective attention tasks during phasic firing, while the performance became poor when LC neurons showed tonic firing (Aston-Jones and Bloom 1981a, 1981b; Aston-Jones and Cohen 2005; Foote et al. 1980; Howells et al. 2012; Rajkowski et al. 1994). Although we did not analyze the firing patterns of LC neurons, the resting membrane potential will change the firing frequency and possibly alter the firing patterns. A depolarized membrane and faster firing frequency in juvenile SHR LC neurons would affect cognitive function in juvenile SHR. RMP and SFR in neonatal LC neurons were not statistically different between SHR and Wistar rats, whereas juvenile and adult SHR showed a significantly

depolarized membrane potential and an increase in SFR when compared with age-matched Wistar rats.

The LC is the major noradrenergic nucleus in the central nervous system (CNS). We examined the involvement of α1- and α2-ARs in the depolarized membrane potential observed in juvenile SHR LC neurons. α1-ARs are Gq-coupled, and have been reported to cause membrane depolarization by both augmentation of a non-selective cationic conductance and inhibition of a potassium conductance (Montell 2005; Wu et al. 2010). Activation of α1-ARs in neurons leads to the production of IP_3 and diacylglycerol (DAG), which mobilizes Ca^{2+} from internal Ca^{2+} stores and Ca^{2+} influx from outside the cell through a non-selective cation channel (NSCC). Our results showed that PE-induced an inward current in juvenile and neonatal SHR, as well as in neonatal Wistar LC neurons, but not in juvenile Wistar LC neurons. The PE-induced inward current of juvenile SHR LC neurons was inhibited by prazosin, as well as by the NSCC channel blockers 2-APB and FFA. 2-APB and FFA are also used as TRP channel blockers. TRP channels can be activated by α1-ARs through the Gq protein. TRP channels are a family of NSCC that can form receptor-operated channels and store-operated channels (Clapham 2003; Clapham et al. 2003; Montell 2005; Venkatachalam and Montell 2007; Wu 2010). PE was reported to activate an unknown cation channel in neonatal rat LC neurons (Williams and Marshall 1987). It is possible that the PE-induced inward current in LC neurons may be due to activation of NSCC. In this study, NSCC blockers revealed a small outward current following inhibition of the PE-induced inward current. Moreover, prazosin, an α1-AR antagonist, in the presence of the α2-AR antagonist, induced an outward current in juvenile SHR LC neurons,

suggesting that α1-AR activity may involve resting membrane potential in juvenile SHR LC neurons. When this intrinsic α1-AR activity is inhibited by NSCC blockers or prazosin, the outward current is revealed. This persistent intrinsic α1-AR activity in juvenile SHR could produce membrane depolarization in LC neurons when compared with juvenile Wistar rats. Moreover, the depolarized membrane potential through α1-AR activation may have induced the increase of spontaneous firing in juvenile SHR LC neurons.

The α2-AR channel is coupled with a G-protein inwardly rectifying potassium (GIRK) channel. α2-AR-activated GIRK channels may also contribute to resting membrane potential in LC neurons. α2-AR activation hyperpolarizes the membrane and leads to a reduction in the firing rate. α2-AR stimulation by NA is known to activate GIRK channels and produce outward currents at membrane potentials positive to Ek (Aghajanian and VanderMaelen 1982; Arima et al. 1998; Williams et al. 1985, 1988). A low concentration of NA (3 μM) induced inward currents in juvenile SHR LC neurons, but not in juvenile Wistar LC neurons. NA (3–100 μM)-induced outward currents in the presence of prazosin in both juvenile SHR and Wistar rat LC neurons that were virtually identical. These results indicate that the α2-AR coupled with the GIRK channel was equivalent in SHR and Wistar rats in juvenile LC neurons. While MPH (30 μM)-induced currents varied from the inward to outward currents in juvenile SHR, all Wistar LC neurons exhibited the outward current. These results suggest that the total current evoked by NA or MPH consists of the sum of α1- and α2-AR-activated currents in juvenile SHR.

Previous studies have confirmed the existence of α1-ARs in brain slice preparations from the adult rat using PCR (Osborne et al. 2002; Pullen et al. 1985). Immunohistochemical results also illustrated the presence of both α1- and α2-ARs in juvenile Wistar and SHR LC neurons, suggesting that the attenuation of functional α1-ARs in developed Wistar LC neurons might relate to loss of secondary messenger. However, the function of α1-ARs in the adult rat LC neurons has not been previously reported. By examining the membrane properties of LC neurons in SHR and Wistar rats in postnatal developmental stages, we found a persistent α1-AR activity in SHR, which disappeared in Wistar rats. It is possible that the delayed maturation may have influenced the persistent α1-AR activity in juvenile SHR. In fact, Shaw et al (2007) reported that human ADHD patients showed delayed maturation of the cortex and striatum. In voltage clamp experiments, we avoided using older SHR (>P35) as they develop hypertension, which might alter the adrenergic system. RMP and SFR were not statistically different between juvenile and adult SHR LC neurons. Nevertheless, we confirmed that LC neurons obtained from older SHRs (P49–56) could also induce hyperpolarization by prazosin as well as for juvenile SHRs. Thus, these data suggest that α1-ARs remain in the older SHR LC neurons.

Activation of α2-ARs improves working memory performance in rats, and α2-AR agonists can improve attention and behavioral inhibition. High levels of noradrenalin release can impair cognitive function through α1-AR activation (Arnsten and Pliszka 2011; Arnsten et al. 2007; Birnbaum et al. 1999). By contrast, α1-AR activation is necessary for MPH-induced improvement in sustained attention (Berridge et al. 2012). Low-dose MPH increases NA in the prefrontal cortex and improves cognitive function

(Berridge et al. 2006; Devilbiss and Berridge 2006). In support of these reports, we demonstrated that stimulation of α1- and α2-ARs has counteracting effects, and that MPH induced an inward current in juvenile SHR LC neurons. LC neurons also project to the prefrontal cortex. Thus, α1-AR activity in LC neurons may affect the release of NA in the prefrontal cortex. Moreover, the α1-AR mRNA levels decrease during postnatal development in SD rats (Nakamura et al. 1988; Osborne et al. 2002; Williams and Marshall 1987). On the other hand, there are some reports that MPH can improve cognitive function in healthy adults (Agay et al. 2010; Camp-Bruno and Herting 1994; Linssen et al. 2011; Smith and Farah 2011; Tomasi et al. 2010). We demonstrated that functional α1-ARs in the LC are attenuated during the developmental period in Wistar rats, while α1-ARs remain functional in other CNS areas including the medial prefrontal cortex (mPFC) in adult animals. The mPFC is a critical area of the cerebral cortex involved in cognitive function (Berridge et al. 2006; Devilbiss and Berridge 2006). Noradrenergic activity at α1-ARs in the mPFC facilitates cognitive performance (Lapiz et al. 2006). Devoto et al. (2005) also demonstrated that electrical stimulation of the LC increased NA and DA in the mPFC using adult SD rats. Therefore, the effects of MPH on cognitive function in healthy adulthood could result from the action of MPH on alpha-NA and/or DA receptors in the mPFC. Cognitive function consists of a variety of higher brain functions including screening targets, sustained attention, working memory, and executive function. NA and DA receptors are involved in these cognitive functions. Of these various functions, some may be improved by α1-AR, α2-AR and DA receptors, while some may not. The role of α1- and α2-ARs and DA receptors in complex cognitive function requires further examination.

In the present study, we demonstrated that functional α1-ARs persisted in juvenile and adult SHR LC neurons, which may cause membrane depolarization and increase spontaneous firing. Although the noradrenergic receptor has three subtypes (α1, α2 and β), in the present study we only focused on the α1- and α2-ARs in LC neurons. The noradrenergic α1-ARs exist primarily at postsynaptic sites, whereas α2-ARs exist at both pre- and postsynaptic sites (Berridge and Waterhouse 2003). Noradrenergic signals are thought to be inhibited by an auto-receptor via an axon-recurrent collateral. Persistent functional α1-ARs in LC neurons and a projecting axon terminal that counteracts α2-ARs in the LC soma could interfere with the auto-receptor. Weakened α2 noradrenergic signaling by persistent α1-AR function could interrupt the action of LC neurons on cognitive function and sustained attention in juvenile SHR.

Acknowledgements

We thank Takayuki Tokimasa and Hiroshi Hasuo for helpful comments and techniques for this experiment.

References

Adriani W, Caprioli A, Granstrem O, Carli M, Laviola G. The spontaneously hypertensive-rat as an animal model of ADHD: evidence for impulsive and non-impulsive subpopulations. *Neurosci Biobehav Rev* 27: 639-651, 2003.

Agay N, Yechiam E, Carmel Z, Levkovitz Y. Non-specific effects of methylphenidate (Ritalin) on cognitive ability and decision-making of ADHD and healthy adults. *Psychopharmacology* 210: 511-519, 2010.

Aghajanian GK, VanderMaelen CP. α_2-Adrenoceptor-mediated hyperpolarization of locus coeruleus neurons: intracellular studies in vivo. *Science* 215: 1394-1396, 1982.

Arima J, Kubo C, Ishibashi H, Akaike N. α_2-Adrenoceptor-mediated potassium currents in acutely dissociated rat locus coeruleus neurones. *J Physiol* 508: 57-66, 1998.

Arnsten AF, Scahill L, Findling RL. alpha2-Adrenergic receptor agonists for the treatment of attention-deficit/hyperactivity disorder: emerging concepts from new data. *J Child Adolesc Psychopharmacol* 17: 393-406, 2007.

Arnsten AFT, Pliszka SR. Catecholamine influences on prefrontal cortical function: relevance to treatment of attention deficit/hyperactivity disorder and related disorders. *Pharmacol Biochem Behav* 99: 211-216, 2011.

Andrus BM, Blizinsky K, Vedell PT, Dennis K, Shukla PK, Schaffer DJ, Radulovic J, Churchill GA, Redei EE. Gene expression patterns in the hippocampus and amygdala of endogenous depression and chronic stress models. *Mol Psychiatry* 17: 49-61, 2012.

Aston-Jones G, Bloom FE. Activity of norepinephrine-containing locus coeruleus neurons in behaving rats anticipates fluctuations in the sleep-waking cycle. *J Neurosci* 1: 876-886, 1981a.

Aston-Jones G, Bloom FE. Norepinephrine-containing locus coeruleus neurons in behaving rats exhibit pronounced responses to non-noxious environmental stimuli. *J Neurosci* 1: 887-900, 1981b.

Aston-Jones G, Cohen JD. An integrative theory of locus coeruleus-norepinephrine function: adaptive gain and optimal performance. *Annu Rev Neurosci* 28: 403-450, 2005.

Aston-Jones G, Shipley MT, Chouvet G, Ennis M, van Bockstaele E, Pieribone V, Shiekhattar R, Akaoka H, Drolet G, Astier B, Charléty P, Valentino RJ, Williams JT. Afferent regulation of locus coeruleus neurons: anatomy, physiology and pharmacology. *Prog Brain Res* 88: 47-75, 1991.

Berridge CW, Devilbiss DM, Andrzejewski ME, Arnsten AFT, Kelley AE, Schmeichel B, Hamilton C, Spencer RC. Methylphenidate preferentially increases catecholamine neurotransmission within the prefrontal cortex at low doses that enhance cognitive function. *Biol Psychiatry* 60: 1111-1120, 2006.

Berridge CW, Shumsky JS, Andrzejewski ME, McGaughy JA, Spencer RC, Devilbiss DM, Waterhouse BD. Differential sensitivity to psychostimulants across prefrontal cognitive tasks: differential involvement of noradrenergic α_1- and α_2-receptors. *Biol Psychiatry* 71: 467-473, 2012.

Berridge CW, Waterhouse BD. The locus coeruleus-noradrenergic system: modulation of behavioral state and state-dependent cognitive processes. *Brain Res Rev* 42: 33-84, 2003.

Birnbaum S, Gobeske KT, Auerbach J, Taylor JR, Arnsten AF. A role for norepinephrine in stress-induced cognitive deficits: alpha-1-adrenoceptor mediation in the prefrontal cortex. *Biol Psychiatry* 46: 1266-1274, 1999.

Camp Bruno JA, Herting RL. Cognitive effects of milacemide and methylphenidate in healthy young adults. *Psychopharmacology* 115: 46-52, 1994.

Clapham DE. TRP channels as cellular sensors. *Nature* 426: 517-524, 2003.

Clapham DE, Montell C, Schultz G, Julius D. International Union of Pharmacology. XLIII. Compendium of voltage-gated ion channels: transient receptor potential channels. *Pharmacol Rev* 55: 591-596, 2003.

Devilbiss DM, Berridge CW. Low-dose methylphenidate actions on tonic and phasic locus coeruleus discharge. *J Pharmacol Exp Ther* 319: 1327-1335, 2006.

Devoto P, Flore G, Saba P, Fà M, Gessa GL. Co-release of noradrenaline and dopamine in the cerebral cortex elicited by single train and repeated train stimulation of the locus coeruleus. *BMC Neurosci* 6: 31-31, 2005.

Foote SL, Aston-Jones G, Bloom FE. Impulse activity of locus coeruleus neurons in awake rats and monkeys is a function of sensory stimulation and arousal. *Proc Natl Acad Sci USA* 77: 3033-3037, 1980.

Howells FM, Stein DJ, Russell VA. Synergistic tonic and phasic activity of the locus coeruleus norepinephrine (LC-NE) arousal system is required for optimal attentional performance. *Metab Brain Dis* 27: 267-274, 2012.

Hurley LL, Akinfiresoye L, Nwulia E, Kamiya A, Kulkarni AA, Tizabi Y. Antidepressant-like effects of curcumin in WKY rat model of depression is associated with an increase in hippocampal BDNF. *Behav Brain Res* 239: 27-30, 2013.

Lapiz MDS, Morilak DA. Noradrenergic modulation of cognitive function in rat medial prefrontal cortex as measured by attentional set shifting capability. *Neuroscience* 137: 1039-1049, 2006.

Linssen AMW, Vuurman EFPM, Sambeth A, Riedel WJ. Methylphenidate produces selective enhancement of declarative memory consolidation in healthy volunteers. *Psychopharmacology* 221: 611-619, 2012.

Montell C. The TRP superfamily of cation channels. *Sci STKE* 272: re3, 2005.

Nakamura S, Sakaguchi T, Kimura F, Aoki F. The role of $alpha_1$-adrenoceptor-mediated collateral excitation in the regulation of the electrical activity of locus coeruleus neurons. *Neuroscience* 27: 921-929, 1988.

Osborne PB, Vidovic M, Chieng B, Hill CE, Christie MJ. Expression of mRNA and functional $alpha_1$-adrenoceptors that suppress the GIRK conductance in adult rat locus coeruleus neurons. *Br J Pharmacol* 135: 226-232, 2002.

Pullen GL, Oltmans GA, Berenbaum SA, Hansen TR. alpha 1-Adrenergic receptor binding in the spontaneously hypertensive rat. *Hypertension* 7: 333-339, 1985.

Rajkowski J, Kubiak P, Aston Jones G. Locus coeruleus activity in monkey: phasic and tonic changes are associated with altered vigilance. *Brain Res Bull* 35: 607-616, 1994.

Russell VA. Reprint of "Neurobiology of animal models of attention-deficit hyperactivity disorder". *J Neurosci Methods* 166: I-XIV, 2007.

Sagvolden T. Behavioral validation of the spontaneously hypertensive rat (SHR) as an animal model of attention-deficit/hyperactivity disorder (AD/HD). *Neurosci Biobehav Rev* 24: 31-39, 2000.

Sagvolden T, Pettersen MB, Larsen MC. Spontaneously hypertensive rats (SHR) as a putative animal model of childhood hyperkinesis: SHR behavior compared to four other rat strains. *Physiol Behav* 54: 1047-1055, 1993.

Shaw P, Eckstrand K, Sharp W, Blumenthal J, Lerch JP, Greenstein D, Clasen L, Evans A, Giedd J, Rapoport JL. Attention-deficit/hyperactivity disorder is characterized by a delay in cortical maturation. *Proc Natl Acad Sci U S A* 104: 19649-19654, 2007.

Smith ME, Farah MJ. Are prescription stimulants "smart pills"? The epidemiology and cognitive neuroscience of prescription stimulant use by normal healthy individuals. *Psychol Bull* 137: 717-741, 2011.

Tomasi D, Volkow ND, Wang GJ, Wang R, Telang F, Caparelli EC, Wong C, Jayne M, Fowler JS. Methylphenidate enhances brain activation and deactivation responses to visual attention and working memory tasks in healthy controls. *NeuroImage* 54: 3101-3110, 2011.

Venkatachalam K, Montell C. TRP channels. *Annu Rev Biochem* 76: 387-417, 2007.

Williams JT, Henderson G, North RA. Characterization of α_2-adrenoceptors which increase potassium conductance in rat locus coeruleus neurones. *Neuroscience* 14: 95-101, 1985.

Williams JT, Marshall KC. Membrane properties and adrenergic responses in locus coeruleus neurons of young rats. *J Neurosci* 7: 3687-3694, 1987.

Williams JT, North RA, Tokimasa T. Inward rectification of resting and opiate-activated potassium currents in rat locus coeruleus neurons. *J Neurosci* 8: 4299-4306, 1988.

Wu L-J, Sweet T-B, Clapham DE. International Union of Basic and Clinical Pharmacology. LXXVI. Current progress in the mammalian TRP ion channel family. *Pharmacol Rev* 62: 381-404, 2010.

Yamada M, Kawahara Y, Kaneko F, Kishikawa Y, Sotogaku N, Poppinga WJ, Folgering JHA, Dremencov E, Kawahara H, Nishi A. Upregulation of the dorsal raphe nucleus-prefrontal cortex serotonin system by chronic treatment with escitalopram in hyposerotonergic Wistar-Kyoto rats. *Neuropharmacology* 72: 169-178, 2013.

Figure Captions

Fig. 1. Representative traces of spontaneous firing of LC neurons from *A*) neonatal (P 3–5), *B*) juvenile (P 21–28) and *C*) adult (P 49–56) rats. Note the reduced firing rate in juvenile and adult Wistar rats, but maintenance of faster firing rate in juvenile and adult SHR.

Fig. 2. Effect of prazosin (500 nM) on membrane potential and spontaneous firing of LC neurons. Representative traces were obtained from *A*) neonatal, *B*) juvenile and *C*) adult rats (Neonatal: Wistar n=8 from five rats, SHR n=8 from four rats; Juvenile: Wistar n=6 from five rats, SHR n=7 from four rats; Adult: Wistar n=7 from four rats, SHR n=5 from four rats). Note that all LC neurons except from juvenile and adult Wistar rats were hyperpolarized by prazosin. Juvenile and adult Wistar LC neurons were prazosin resistant.

Fig. 3. Effect of prazosin (500 nM) on membrane current of LC neurons. Representative traces of prazosin-induced current from *A*) neonatal and *B*) juvenile animals in the presence of yohimbine (1 μM) and TTX (1 μM). Prazosin-induced an outward current in all LC neurons, except from juvenile Wistar rats. *C*) Summary of prazosin-induced outward currents (Neonatal: Wistar n=7 from four rats, SHR n=7 from four rats; Juvenile: Wistar n=8 from four rats, SHR n=7 from four rats). Juvenile Wistar LC neurons showed a significantly small outward current. Data are mean±SE. $^{**}P<0.01$.

Fig. 4. Effect of phenylephrine (PE, 30 μM) on membrane current of LC neurons from *A*) neonatal and *B*) juvenile rats. Voltage clamp recordings were performed at a Vh -60 mV. The bar indicates the period of superfusion. PE in presence of yohimbine (1 μM) and TTX (1 μM) induced an inward current in neonatal and juvenile SHR LC neurons, but not in juvenile Wistar rat LC neurons. *C*) Summary of PE-induced inward currents (Neonatal: Wistar n=10 from six rats, SHR n=16 from nine rats; Juvenile: Wistar n=15 from four rats, SHR n=21 from six rats). Data reported as mean±SE. $^{**}P<0.01$.

Fig. 5. Effect of α1-AR and NSCC antagonists on the PE-induced inward current. *A*) Prazosin terminated PE-induced inward current. NSCC antagonists *B*) 2-APB and FFA abolished the PE-induced inward current in juvenile SHR LC neurons. *C*) Summary of effect of test drugs on PE-induced inward currents. Each column represents the mean±SE (prazosin n=8 from five rats, 2-APB n=9 from four rats, FFA n=8 from four rats).

Fig. 6. Effect of noradrenaline (NA) on the membrane current of LC neurons. *A*) Current recordings from juvenile Wistar LC neurons and *B*) juvenile SHR LC neurons. *C*) Concentration response curve of NA-induced outward currents. The amplitudes of outward currents were 29.9±0.6, 48.7±2.6, 94.4±6.5, 107.8±6.3 and 108.7±10.1 pA in juvenile Wistar rat LC neurons and 13.5±0.4, 44.7±2.6, 73.2±10.4, 77.8±5.9 and 83.5± 2.7pA in juvenile SHR LC neurons following application of 3, 10, 30, 100 and 300 μM of NA, respectively. *D*) Concentration response curve of NA-induced outward current in the presence of prazosin (500 nM). The amplitudes of outward currents were 21.6±3.3, 61.6±2.9, 100.5±15.2 and 125.7±11.9 pA in juvenile Wistar rat LC neurons

and 21.6±1.7, 60.2±2.3, 102.7±10.8 and 118.8±8.7 pA in juvenile SHR LC neurons following application of 3, 10, 30 and 100 μM of NA, respectively. Each point represents the mean±SE obtained from 4–8 LC neurons. Differences between Wistar (●) and SHR (○) rats at specific concentrations were analyzed by Student's unpaired *t*-test. **P*<0.05, ***P*<0.01. *E*) Summary of the effect of methylphenidate (30 μM) on the membrane current of juvenile LC neurons. (Wistar *n*=15 from five rats, SHR *n*=15 from six rats). ***P*<0.01.

Fig. 7. Confocal micrographs from horizontal LC sections. Sections were triple stained for TH (*a, d red*), α1A and α2B-AR (*b, e green*) and nuclei (*blue*). Location of α1A and α2B-AR within a field of dense TH neurons in both rats. *c* and *f*) Merged image. Scale bar, 100 μM.

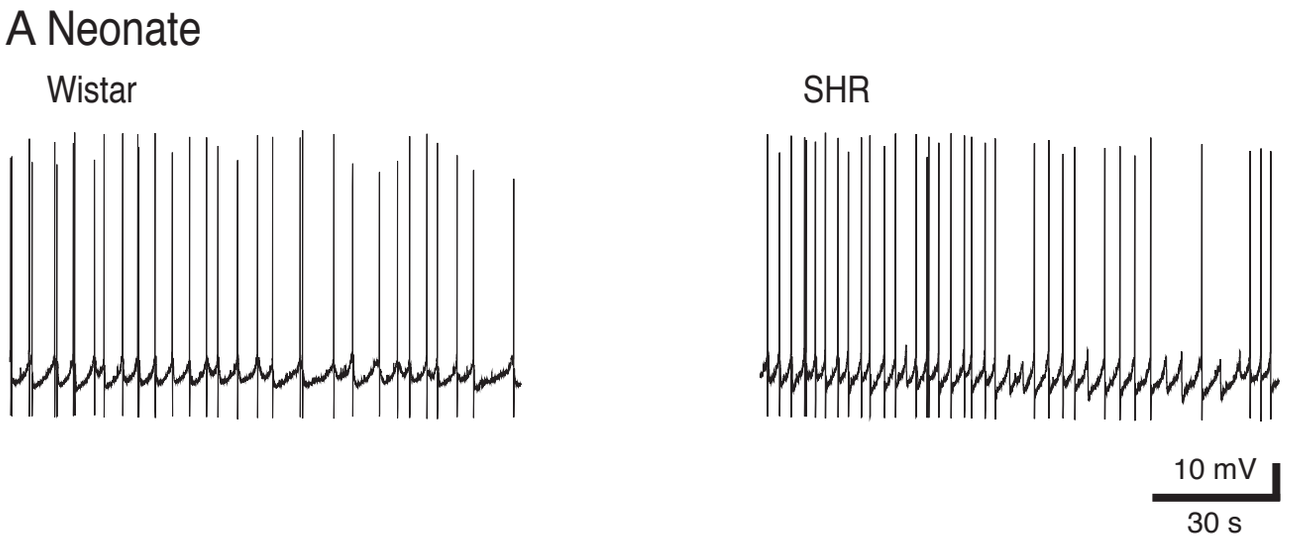
A Neonate
Wistar
SHR
10 mV
30 s
B Juvenile
Wistar
SHR
10 mV
30 s
C Adult
Wistar
SHR
10 mV
30 s

Figure 1

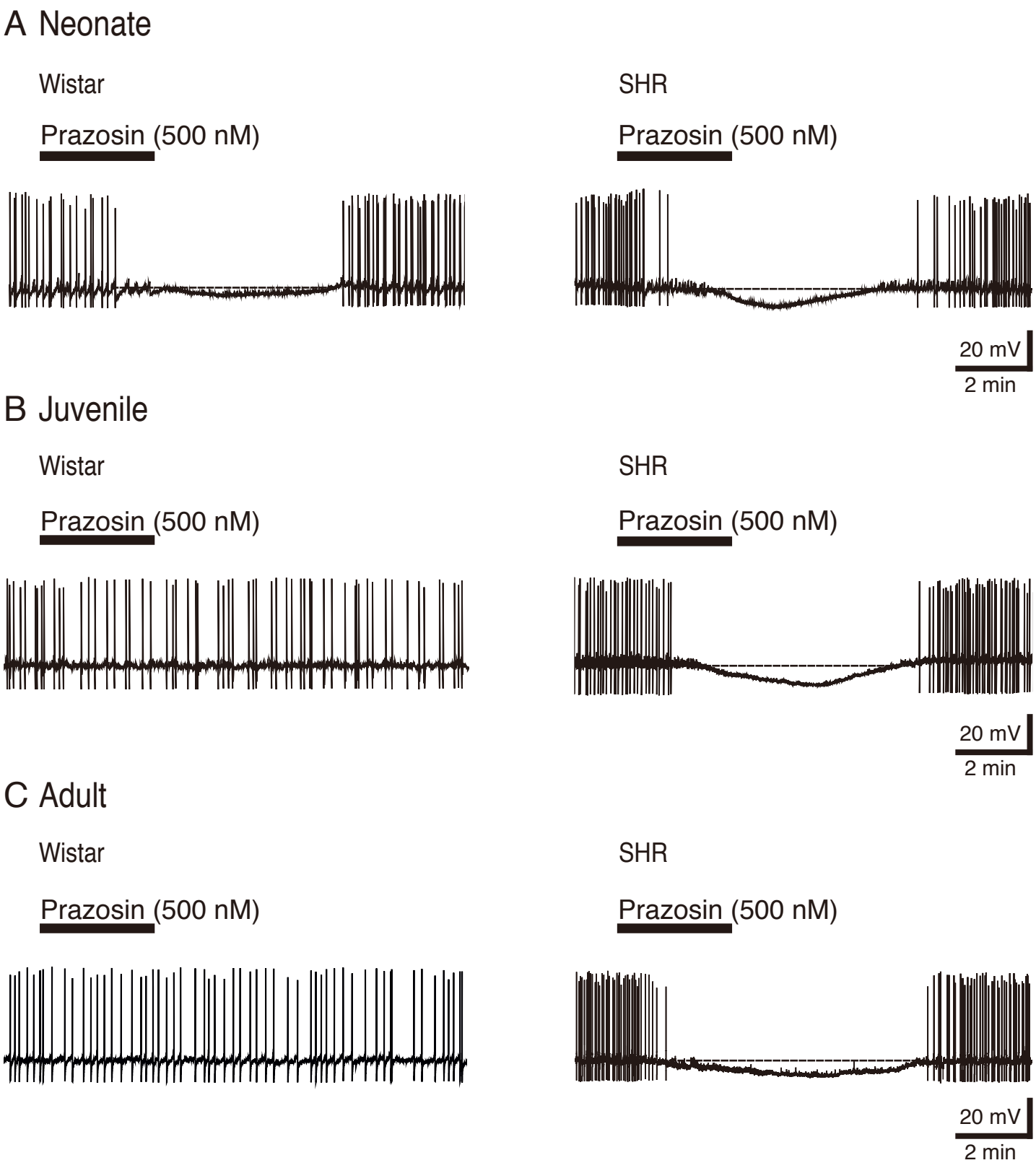
A Neonate
Wistar
Prazosin (500 nM)
SHR
Prazosin (500 nM)
20 mV
2 min
B Juvenile
Wistar
Prazosin (500 nM)
SHR
Prazosin (500 nM)
20 mV
2 min
C Adult
Wistar
Prazosin (500 nM)
SHR
Prazosin (500 nM)
20 mV
2 min

Figure 2

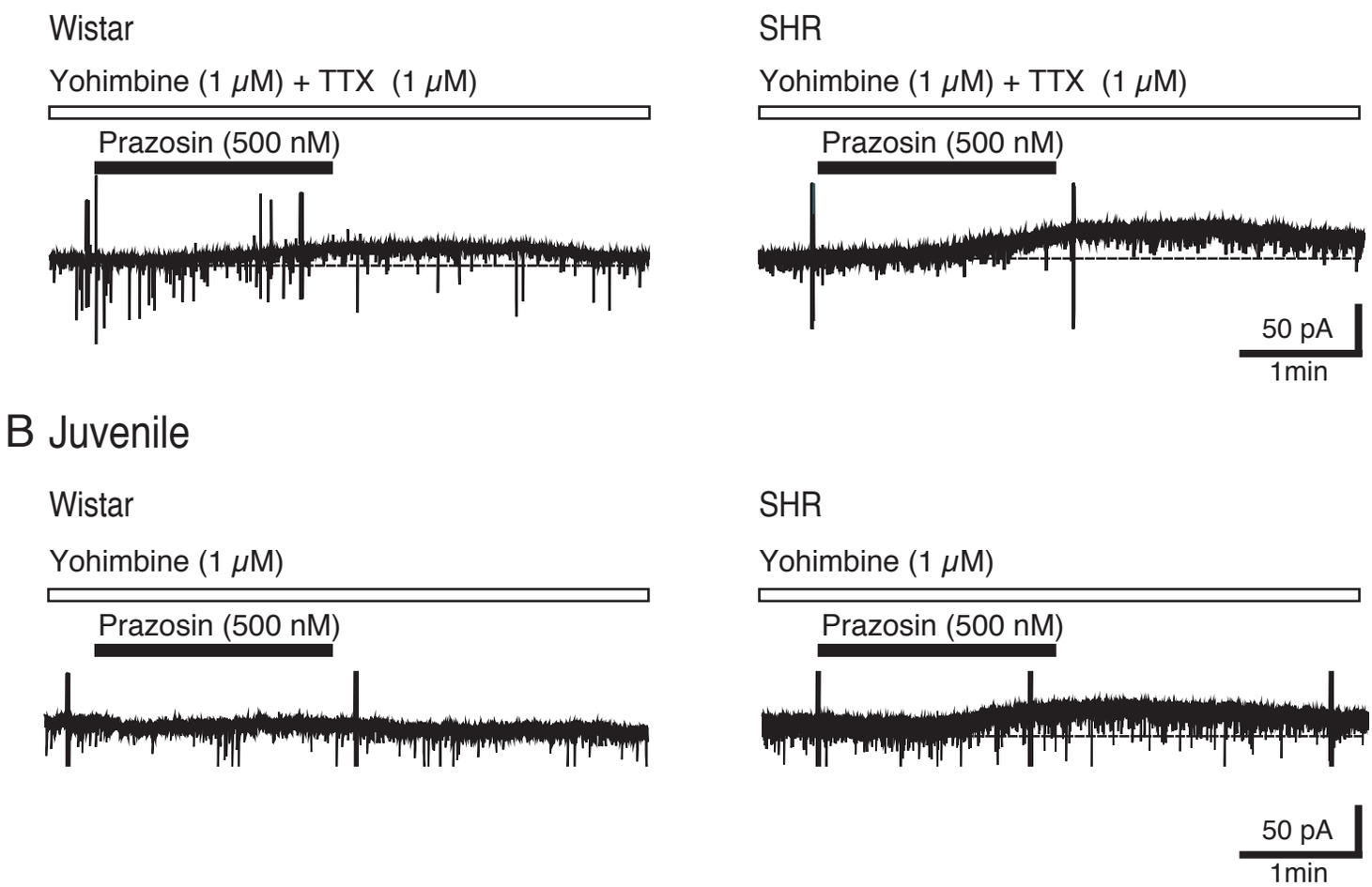
A Neonate
Wistar
Yohimbine (1 μM) + TTX (1 μM)
Prazosin (500 nM)
SHR
Yohimbine (1 μM) + TTX (1 μM)
Prazosin (500 nM)
50 pA
1min
B Juvenile
Wistar
Yohimbine (1 μM)
Prazosin (500 nM)
SHR
Yohimbine (1 μM)
Prazosin (500 nM)
50 pA
1min

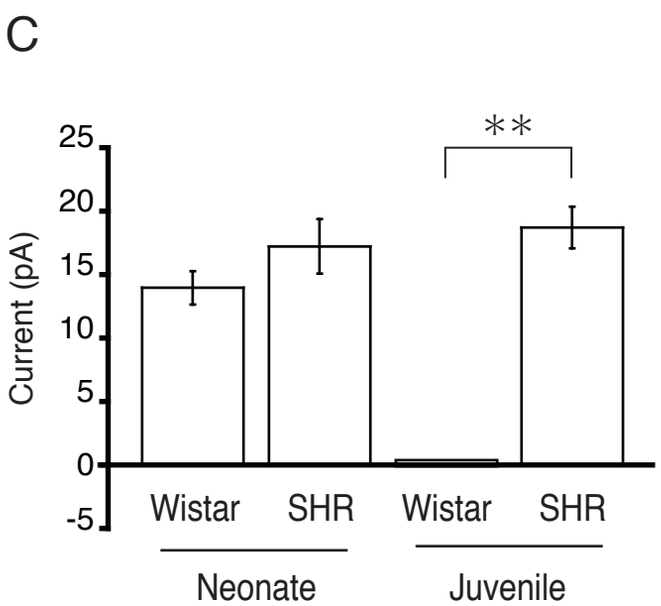
C
**
25
20
15
10
5
0
-5
Current (pA)
Wistar
SHR
Wistar
SHR
Neonate
Juvenile

Figure 3

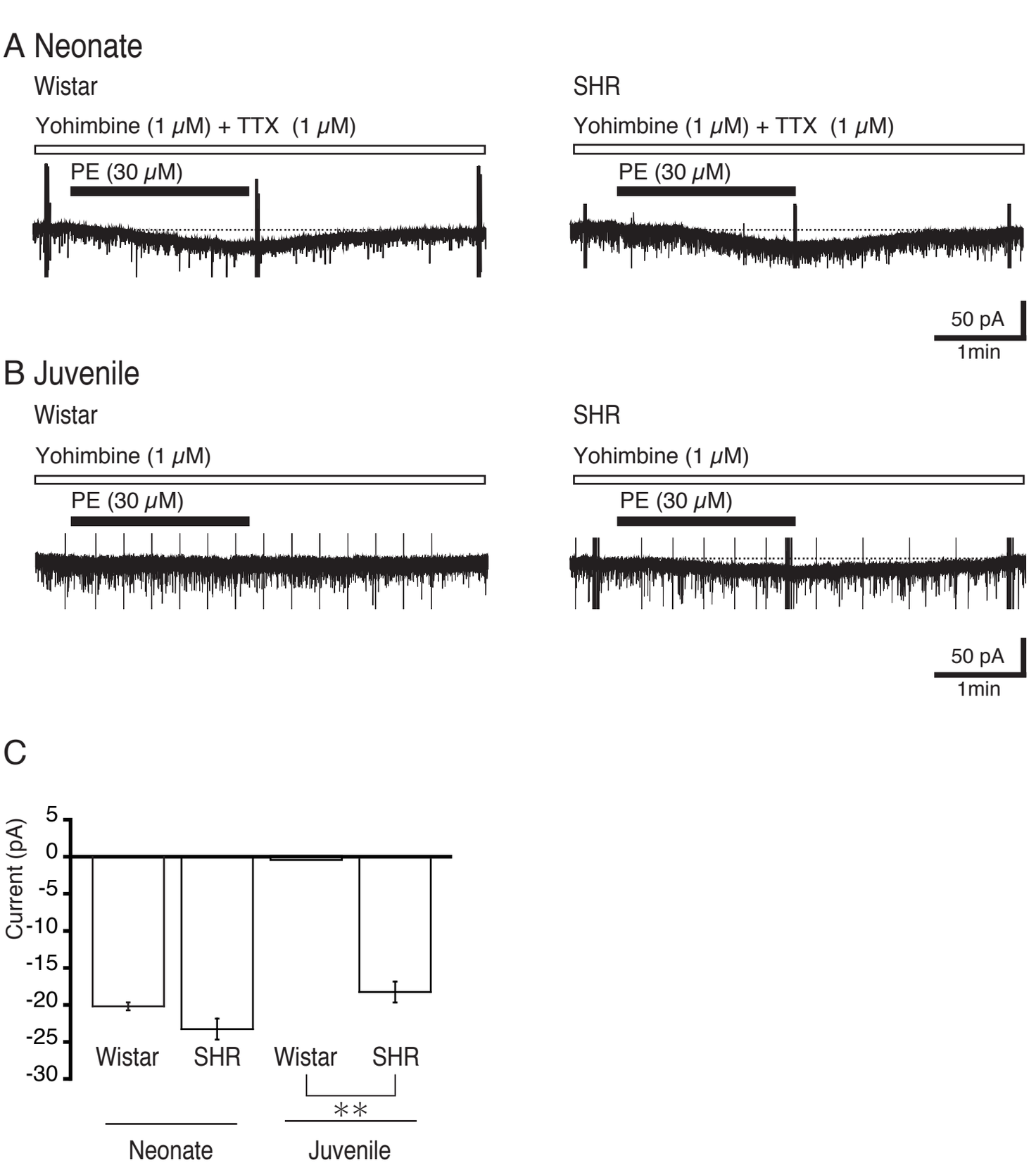
A Neonate
Wistar
Yohimbine (1 μM) + TTX (1 μM)
PE (30 μM)
SHR
Yohimbine (1 μM) + TTX (1 μM)
PE (30 μM)
50 pA
1min
B Juvenile
Wistar
Yohimbine (1 μM)
PE (30 μM)
SHR
Yohimbine (1 μM)
PE (30 μM)
50 pA
1min
C
Current (pA)
5
0
-5
-10
-15
-20
-25
-30
Wistar
SHR
Wistar
SHR
**
Neonate
Juvenile

Figure 4

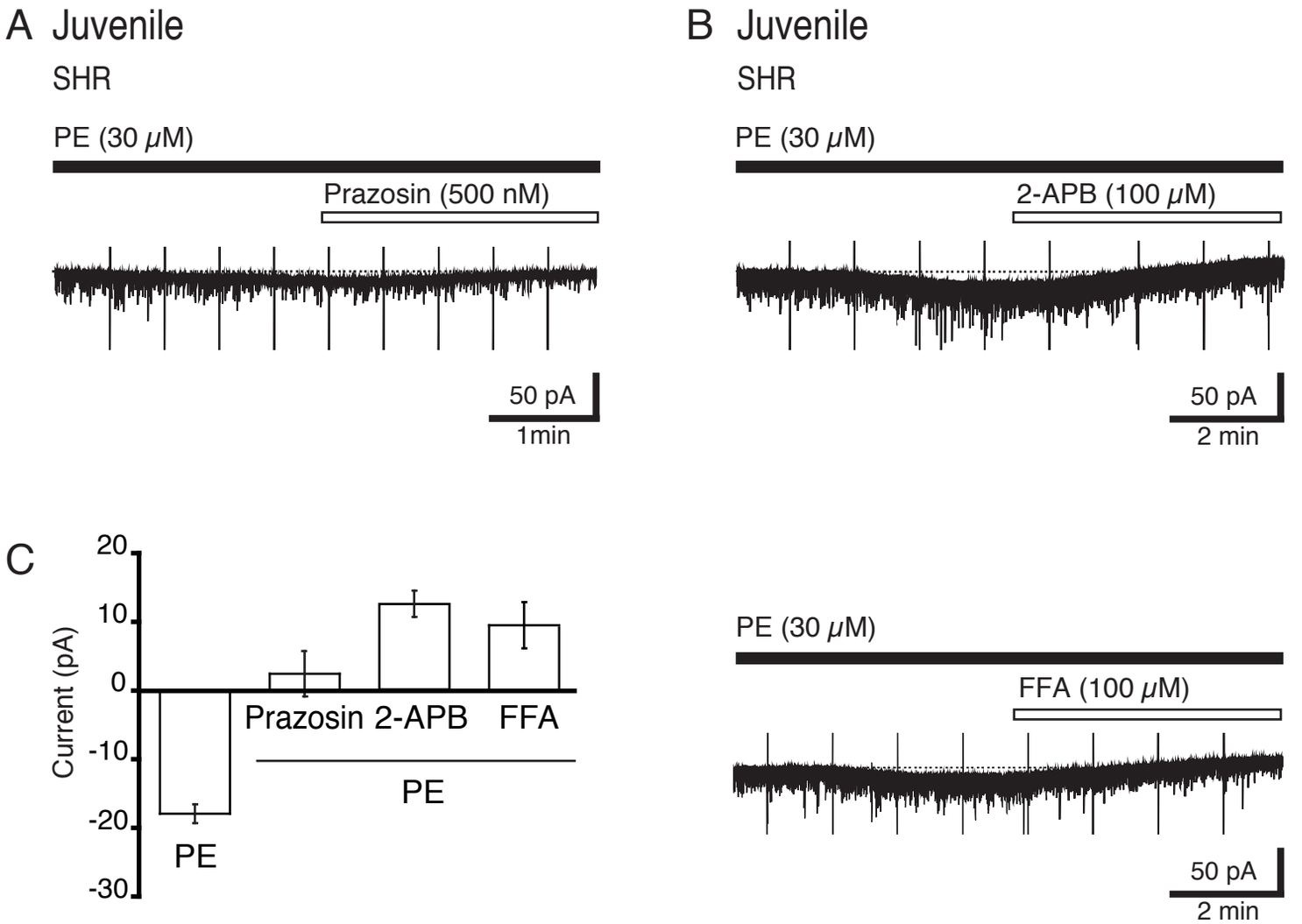
A Juvenile
SHR
PE (30 μM)
Prazosin (500 nM)
50 pA
1min
B Juvenile
SHR
PE (30 μM)
2-APB (100 μM)
50 pA
2 min
C
Current (pA)
20
10
0
-10
-20
-30
Prazosin
2-APB
FFA
PE
PE
PE (30 μM)
FFA (100 μM)
50 pA
2 min

Figure 5

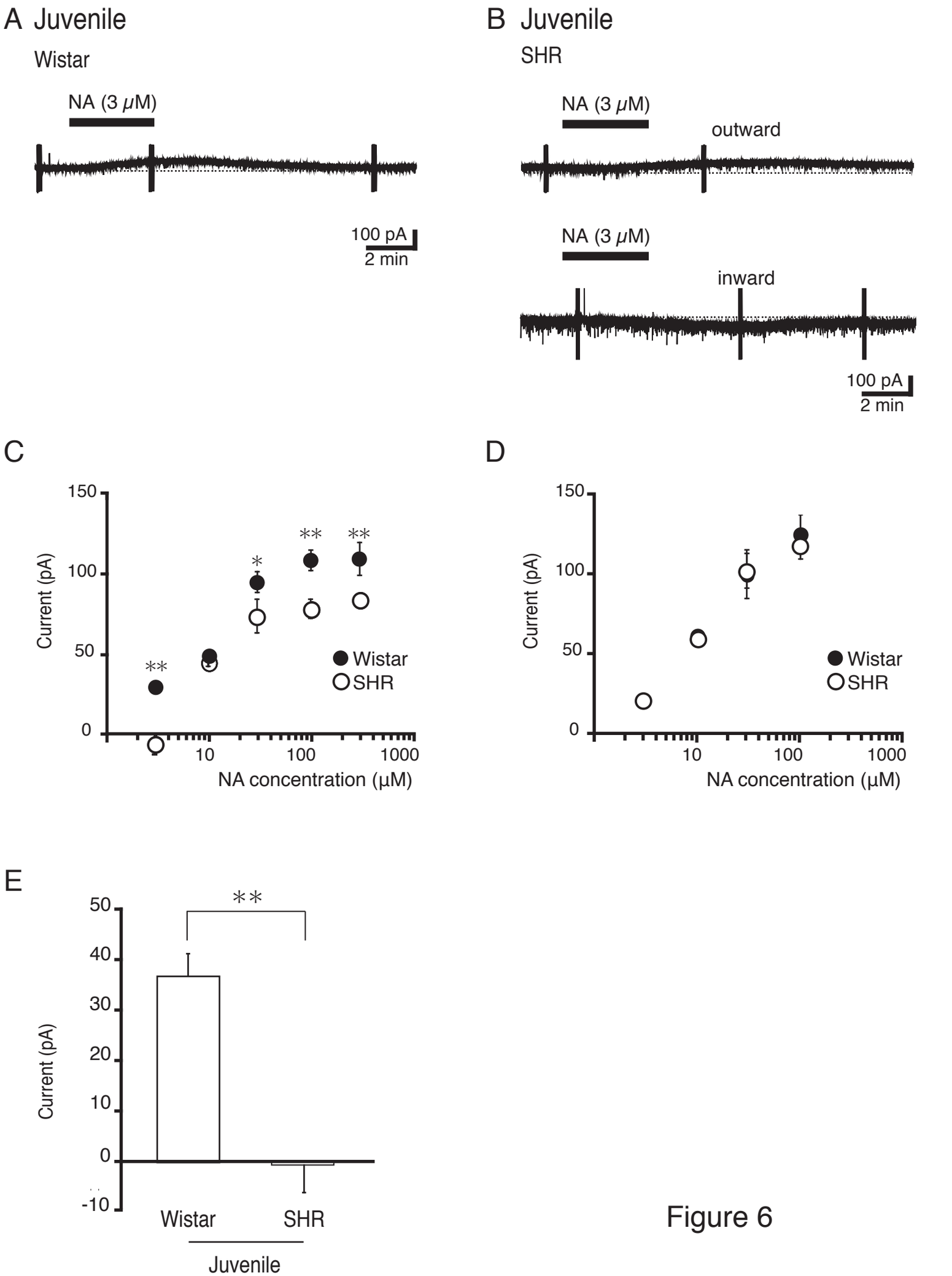
A Juvenile
Wistar
NA (3 μM)
100 pA
2 min
B Juvenile
SHR
NA (3 μM)
outward
NA (3 μM)
inward
100 pA
2 min
C
Current (pA)
150
100
50
0
10
100
1000
NA concentration (μM)
Wistar
SHR
D
Current (pA)
150
100
50
0
10
100
1000
NA concentration (μM)
Wistar
SHR
E
Current (pA)
50
40
30
20
10
0
-10
Wistar
SHR
Juvenile

Figure 6

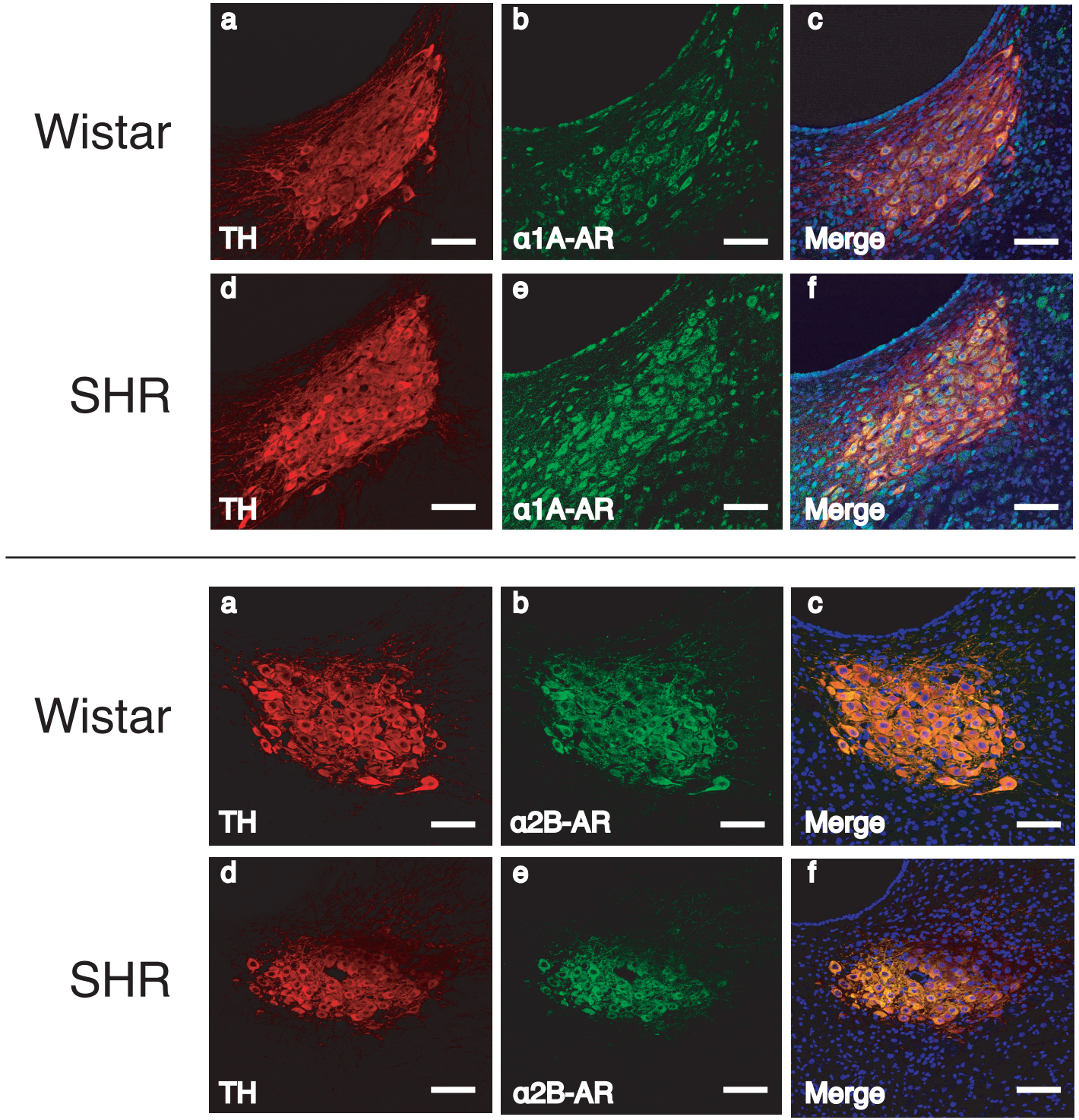
Wistar
SHR
a
b
c
d
e
f
TH
α1A-AR
Merge
Wistar
SHR
a
b
c
d
e
f
TH
α2B-AR
Merge

Figure 7